# Insight into the mechanism of the IMP-1 metallo-β-lactamase by molecular dynamics simulations

Peter Oelschlaeger[1,2], Rolf D. Schmid[1], Jürgen Pleiss[1,3]

[1]Institute of Technical Biochemistry, University of Stuttgart, Allmandring 31, 70569 Stuttgart, Germany

[2]Present adress: Mayo Group, Division of Biology, Mail Code 114-96, California Institute of Technology, Pasadena, CA 91125

[3]Communicating author:
Dr. Jürgen Pleiss
Institute of Technical Biochemistry
University of Stuttgart
Allmandring 31
D-70569 Stuttgart, Germany
Email: itbjpl@po.uni-stuttgart.de
Fax: +49-711-685-3196
Phone: +49-711-685-3191

Running title: MD simulations of IMP-1 metallo-β-lactamase

Keywords: metalloprotein/metallo-β-lactamase/molecular dynamics simulation/ zinc coordination/β-lactam hydrolysis

Abbreviations: MD, molecular dynamics; RMSD, root mean square deviation

## Abstract

Two models, a purely nonbonded model and a cationic dummy atom approach, were examined for the modeling of the binuclear zinc-containing IMP-1 metallo-β-lactamase in complex with a mercaptocarboxylate inhibitor. The cationic dummy atom approach had substantial advantages as it maintained the initial, experimentally determined geometry of the metal-containing active site during molecular dynamics simulations in water. The method was extended to the modeling of the free enzyme and the enzyme in complex with a cephalosporin substrate docked in an intermediate structure. For all three systems, the modeled complexes and the tetrahedral coordination of the zinc ions were stable. The average zinc-zinc distance increased by about 1 Å in the substrate complex compared to the inhibitor complex and the free enzyme in which a hydroxide ion acts as a bridging ligand. Thus, the zinc ions are predicted to undergo a back and forth movement upon the cycle of hydrolysis. In contrast to previous assumptions, no interaction of the Asn167 side chain with the bound cephalosporin substrate was observed. Our observations are in agreement with quantum-mechanical calculations and experimental data and indicate that the cationic dummy atom approach is useful to model zinc-containing metallo-β-lactamases as free proteins, in complex with inhibitors and in complex with substrates.

# Introduction

β-Lactam antibiotics have a cytostatic effect on bacteria by binding irreversibly to a transpeptidase involved in cell wall peptidoglycan polymerization (Lee *et al.*, 2001; Green, 2002) and are widely used for the treatment of infectious diseases. β-Lactamases [E.C. 3.5.2.6] hydrolyze these antibiotics and thus confer resistance to bacteria. β-Lactamases have been grouped into four homologous classes (Ambler, 1980): classes A, C and D use a serine-dependent mechanism and have been investigated intensively (Matagne *et al.*, 1998; Petrosino *et al.*, 1998); class B β-lactamases use a completely different mechanism for the hydrolysis of β-lactams. They contain either one or two zinc ions and are also known as metallo-β-lactamases. A hydroxide ion, coordinated to one or two zinc ions, is believed to be the nucleophilic agent (Wang *et al.*, 1999; Suárez and Merz, 2001). From studies on the mechanism of nitrocefin hydrolysis catalyzed by the binuclear *Bacteroides fragilis* metallo-β-lactamase (Wang *et al.*, 1999), protonation of an intermediate was identified as the rate-limiting step. The intermediate results from hydrolysis of the β-lactam ring and binds to both catalytic zinc ions: to one zinc via the carboxyl group resulting from the hydrolysis of the amide bond, to the other zinc via the anionic nitrogen emerging from the amide hydrolysis. This structure is then broken down by protonation and release of the product. Subsequently, the catalytic cycle starts again by binding of a hydroxide to the enzyme as a bridging ligand between the two zinc ions. Metallo-β-lactamases are capable of hydrolyzing a broad spectrum of β-lactams such as penicillins, cephalosporins and carbapenems. Due to this broad substrate spectrum and their insensitiveness toward natural inhibitors like clavulanic acid (Liras and Rodriguez-Garcia, 2000) and synthetic inhibitors which inactivate serine-β-lactamases (Heinze-Krauss *et al.*, 1998; Hubschwerlen *et al.*, 1998; Ness *et al.*, 2000; Kaur *et al.*, 2001), they have become a serious problem in nosocomial strains in Japan (Laraki *et al.*, 1999),

China (Hawkey *et al.*, 2001) and Italy (Riccio *et al.*, 2000). Inhibitors, which act on metallo-β-lactamases are mainly electron donors which coordinate to one or two zinc ions of the enzyme, such as biphenyl tetrazoles (Toney *et al.*, 1998), thiol compounds (Concha *et al.*, 2000; Huntley *et al.*, 2000), thioesters, that are hydrolyzed to thiol compounds (Hammond *et al.*, 1999; Mollard *et al.*, 2001) or succinic acids (Toney *et al.*, 2001).

Molecular modeling can assist in understanding properties of metallo-β-lactamases and their interaction with substrates, and in designing of new β-lactams which are not converted. However, the simulation of structure and dynamics of proteins containing transition metals remains a challenge. To model the coordination of zinc ions and ligands in molecular mechanics force fields, either bonded or nonbonded interactions can be used. In bonded approaches (Merz *et al.*, 1991; Vedani and Huhta, 1990), the ligands are treated as covalently bound to zinc atoms with force field parameters defining bond length, bond angles and dihedrals. In nonbonded models, ligands and zinc ions only interact via electrostatic and van der Waals forces. In the purely nonbonded approach, the total formal charge of the transition metal is assigned to the center of the atom (Vedani and Huhta, 1990; Stote and Karplus, 1995). However, both approaches have serious limitations: the use of covalent bonds in the bonded approach rigidifies the conformation of the active site (Vedani and Huhta, 1990; Pang *et al.*, 2000) and thus prevents flexibility. The purely nonbonded approach, on the other hand, is frequently not able to obtain tetrahedral zinc coordination (Pang *et al.*, 2000; Berweger *et al.*, 2000; Toba *et al.*, 1999; Vedani *et al.*, 1986). Aquist and Warshel (Aquist and Warshel, 1990) devised a method for modeling transition metals (Mn(II) ions) more authentically than by using a purely nonbonded approach: six fractional positive charges, mimicking the $4s4p^3 4d^2$ orbitals were arranged in octahedral geometry around the center of the ion and, thus, allowed octahedral coordination of ligands. In analogy, a model called "cationic dummy atom approach" has been developed (Pang, 1999) and applied successfully for molecular dynamics (MD) simulations of mononuclear (Pang *et al.*, 2000) and binuclear

zinc-containing proteins (Pang, 2001). In this approach, the zinc´s $4s4p^3$ orbitals that accept electron density of the four ligands (Roe and Pang, 1999) are modeled by four dummy atoms which are arranged tetrahedrally around the zinc atom and carry a partial charge of +0.5 e each. These dummy atoms have been shown to keep the ligands in the correct orientation, enabling a stable simulation of the tetrahedral coordination of the zinc atom (Pang, 1999; Pang *et al.*, 2000; Pang, 2001).

As zinc-containing proteins are of increasing biological interest, a number of them have been simulated: alcohol dehydrogenase (Ryde, 1995) (bonded approach), carboxypeptidase A and a carbonic anhydrase (Stote and Karplus, 1995) (purely nonbonded approach), metalloproteinase (Pang, 1999), farnesyltransferase (Pang *et al.*, 2000), and phosphotriesterase (Pang, 2001) (cationic dummy atom approach). Among the zinc-containing metallo-β-lactamases, the mononuclear enzyme from *Bacillus cereus* (Carfi *et al.*, 1995) was simulated with a bonded approach (Díaz *et al.*, 2001; Suárez and Merz, 2001). The binuclear metallo-β-lactamase from *Bacteroides fragilis* (Concha *et al.*, 1996) was modeled using a mixed bonded and nonbonded approach, with the amino acid ligands and the bridging hydroxide treated as bonded and a water coordinating to Zn2 treated as nonbonded. Changes of loop conformation were observed upon binding of an inhibitor (Salsbury *et al.*, 2001). Recently, for this lactamase different protonation states of Asp103 were investigated (Suarez *et al.*, 2002). Here, either the bridging hydroxide of the free enzyme was bound explicitly to both zincs but not the water molecule, or the hydroxide was only bound to Zn1 and the water molecule to Zn2.

As bonded approaches rigidify the conformation of the active site (Vedani and Huhta, 1990; Pang, 2000) and we wanted to observe subtle dynamic effects, we compared the purely nonbonded model with the cationic dummy atom approach in MD simulations of the binuclear IMP-1 metallo-β-lactamase from *Pseudomonas aeruginosa* in complex with a

mercaptocarboxylate inhibitor and extended the latter approach to IMP-1 as a free enzyme and in complex with a cephalosporin substrate.

# Computational methods

The IMP-1 metallo-β-lactamase from *Pseudomonas aeruginosa* in complex with a mercaptocarboxylate inhibitor has been crystallized and resolved to 2.0 Å (PDB entry 1DD6) (Concha *et al.*, 2000). The coordinates of molecule A, the corresponding inhibitor and crystal water were used for modeling. If not mentioned otherwise, charges of titratable groups were assigned as suggested by the program *PROTONATE* of the *AMBER 6.0* software package (Case *et al.*, 1999) at pH 7.0. His19 was changed from the δ- to the ε-protonated tautomer, thus allowing hydrogen bonds to the backbone of Val36 and Ile47.

## The active site in the purely nonbonded approach

The ligating amino acids Asp81 and Cys158 were deprotonated, His77, His79, His139, and His197 were neutral. In order to coordinate to Zn1, His79 was changed to the ε-protonated tautomer. Several values have been suggested for the van der Waals parameters of zinc ions in nonbonded models (σ = 0.69 Å, ε = 0.014 (Terp *et al.*, 2000), $\sigma$ = 1.45 Å, ε = 0.025 kcal/mol (Wasserman and Hodge, 1996), σ = 1.95 Å and ε = 0.25 kcal/mol (Stote and Karplus, 1995)). The latter were selected for this work. The formal charge of the zincs was +2 e. The inhibitor was built with the *MolBuilder* module of the *InsightII* software (Accelrys, San Diego, CA) and minimized with the *AMPAC/MOPAC* module of *InsightII*. Force field parameters for protein and inhibitor were derived from the *AMBER* libraries (parm96 version of the all-atom *AMBER* force field (Cornell *et al.*, 1995)). The thiol group of the inhibitor was treated as deprotonated, its carboxyl group as either protonated or deprotonated. Electrostatic potentials were calculated quantum-mechanically with the *Gaussian 98* software (Gaussian, Carnegie, PA, level of theory: HF, basis set: 6-31G*) and fitted with the *RESP* program of the *AMBER 6.0* software package.

## The active site in the cationic dummy atom approach

Zinc with dummy atoms was created as reported (Pang *et al.*, 2000). This procedure also includes the deprotonation of titratable groups in the first coordination sphere of zinc ions and protonation of the second coordination sphere. Accordingly, Asp81 and Cys158 were deprotonated. Based on *ab initio* calculations, it has been shown that the proton dissociation energy of imidazole when coordinated to $Zn^{2+}$ is dramatically reduced, suggesting the existence of imidazolate as zinc ligand in proteins (Yazal and Pang, 1999). There is also experimental evidence for histidinate as zinc ligand in proteins (Huang *et al.*, 1996; Trainer *et al.* 1982). Therefore, His77, His79, His139 and His197 were treated as histidinates. Electrostatic potentials of histidinate were taken from Pang et al. (Pang *et al.*, 2000). In accordance with this model, the thiol group of the inhibitor and the carboxyl group resulting from hydrolysis of the amide bond in cephalothin were deprotonated (first coordination sphere); Asp170 was protonated (second coordination sphere). The latter can be interpreted as an acceptor for the proton from His79. For the carboxyl group of the inhibitor, both the deprotonated and protonated form are possible. Thus, both protonation states were investigated.

The free enzyme was created by replacing the inhibitor by a hydroxide ion, for which the parameters were taken from Pang *et al.* (Pang, 2001). In cephalothin, the carboxyl group at the six-membered dihydro-thiazine ring was protonated, as it belongs to the second coordination sphere. Besides, this residue can be considered as an acceptor for the proton of the carboxyl group resulting from amide bond hydrolysis. Minimization, calculation of the electrostatic potentials and parameterization were done as described above. After removal of the inhibitor, the hydrolyzed cephalothin was manually docked into the active site guided by the structure of the inhibitor. The anionic nitrogen resulting from the hydrolyzed amide bond

was coordinated to Zn2 and one oxygen of the respective carboxylate to Zn1. The (2-thiophenyl-1-acetyl)amino residue of cephalothin was oriented according to the 2-phenyl-1-ethyl residue of the inhibitor, and the methylethanoate group according to the (5-methylene-1-tetrazole)-2-thiophenyl residue of the inhibitor (Figure 1).

Using the *xLEaP* program of the *AMBER 6.0* software package, all structures were solvated with a truncated octaeder of TIP3P water with a minimal distance of 10.0 Å between the wall and the protein, and neutralized with $Na^+$ or $Cl^-$ counter ions.

## MD simulation

MD simulations were performed using the *Sander* program of the *AMBER 6.0* software package. *Sander* uses the Particle Mesh Ewald algorithm, equaling a nonbonded cutoff for electrostatics. The cutoff for van der Waals interactions was 8 Å. The resulting systems consisted of about 25,000 atoms. They were energy minimized for 1000 steps (500 steepest descent, 500 conjugate gradient) and heated by MD simulation to 300 K starting at 10 K. The time step was 1 fs and the *SHAKE* algorithm (van Gunsteren and Berendsen, 1977) was applied to all bonds containing hydrogen atoms. The free enzyme was modeled with the *SHAKE* algorithm applied to all bonds. When only applying the SHAKE algorithm to bonds containing hydrogen atoms, coordinate resetting could not be accomplished in this case. During the minimization and heating, the positions of the zinc ions, the inhibitor, the substrate, and the hydroxide were constrained. This prevented the two zinc ions from instantaneously drifting apart in the purely nonbonded approach and allowed the formation of a stable tetrahedral coordination of the zinc ions in the cationic dummy atom approach. When a temperature of 300 K was reached, the constraints were gradually decreased, and the system was equilibrated by unconstrained MD simulations until the root mean square deviations (RMSD) of the backbone atoms from the initial structure were stable. Total simulation times

were 500 ps (purely nonbonded model), 1.6 and 1.75 ns (cationic dummy atom model with deprotonated and protonated inhibitor, respectively), 1 ns (free enzyme), and 2ns (IMP-1 in complex with cephalothin).

## Analysis

To examine the geometry of the active site, average structures were generated over 10 ps intervals using the *ptraj* program of the *AMBER 6.0* software package. The 10 ps intervals were at 490-500 ps (IMP-1/inhibitor with the purely nonbonded approach), 1590-1600 ps and 1740-1750 ps (IMP-1/inhibitor with the cationic dummy atom approach and deprotonated and protonated inhibitor, respectively), 1050-1060 ps (free enzyme) and 1190-1200 ps (IMP-1/cephalothin) of unconstrained simulation time. Distances between Zn1 and Zn2, the zinc ions and the ligands and the angles ligand-zinc-ligand were measured in the average structures with *InsightII*. RMSD between the modeled structures and the initial structure, and distances between Zn1 and Zn2, Lys161 side chain nitrogen and the carboxyl oxygens of the inhibitor or the substrate, and Asn167 side chain nitrogen and the free oxygen of the carboxylate of the substrate were monitored over the course of the simulations using *ptraj*. As the oxygens of the carboxyl groups alternated in forming the salt bridge to the Lys161 side chain nitrogen, the arithmetic mean of the two distances was calculated. Visual inspection of the trajectories was done with the *VMD Viewer* software (Humphrey *et al.*, 1996).

# Results

## IMP-1 in complex with inhibitor

To evaluate the structure and dynamics of the binuclear IMP-1 metallo-β-lactamase in complex with a mercaptocarboxylate inhibitor in MD simulations, three systems were compared: a purely nonbonded model, a model using the cationic dummy atom approach and deprotonated inhibitor, and the same model with protonated inhibitor. An appropriate force field should maintain the experimental structure in a simulation at 300 K without restraints. To test this, average structures of the three systems were generated at the end of the simulations, when the complexes were stable as concluded from the RMSD and the Zn1-Zn2 distances (Figure 2). The average structures were compared to the crystal structure, and the geometry of the active site was analyzed.

In the crystal structure, the two zinc ions are at a distance of 3.6 Å, the distances between the ligands and the zincs are between 2.1 and 2.4 Å. The sulfur atom of the inhibitor acts as a bridging ligand between both zinc ions (Figure 3). Both zinc ions have the coordination number 4: Zn1 is coordinated by three histidines (His77, His79 and His139) and the hydroxide, Zn2 by one oxygen of Asp81, Cys158, His197, and also the hydroxide. The ligand-zinc-ligand angles are all close to the tetrahedral angle of 109.5° with values ranging from 100° to 125°.

The average structure obtained from the purely nonbonded model over 10 ps at the end of the 500 ps simulation differed significantly from this geometry (Figure 3). Only the thiolate group of the inhibitor remained located between the two zinc ions acting as a bridging ligand, and the carboxyl group of the inhibitor remained oriented towards Lys161. However, distances and angles in the active site deviated considerably from the crystal structure: 1) the zinc-zinc distance had increased by 1.1 Å relative to the crystal structure (Figures 2B and 3),

2) the ligand-zinc distances had increased from 2.1-2.4 Å to 2.7-3.0 Å, and 3) the ligand-zinc-ligand angles had changed by up to 47° relative to the crystal structure, ranging from 67° to 160°. In addition, the coordination number 4 of both zinc ions was not maintained, and additional ligands entered into their first coordination spheres: the sulfur atom of Cys158 now functioned as a bridging ligand between the two zinc ions, resulting in a coordination number of 5 for Zn1; the second oxygen atom of Asp81, an oxygen atom of the carboxyl group of the inhibitor, and the side chain oxygen of Ser196 had entered into the first coordination sphere of Zn2, changing its coordination number to 7.

A better representation of the active site was obtained using cationic dummy atom models, with either deprotonated or pronated inhibitor. In both models, the distances between Zn1 and Zn2 (Figure 2D and F), both zinc ions and the ligands, and the ligand-zinc-ligand angles (data not shown) were stable. Average structures of the last 10 ps of the simulations (Figure 4) demonstrate that these geometric parameters deviated less from the crystal structure than in the purely nonbonded model: 1) the zinc-zinc distance had increased by only 0.2 Å (Figures 2D and F), 2) the ligand-zinc distances had decreased from 2.1-2.4 Å to 1.9-2.1 Å, and 3) the ligand-zinc-ligand angles had changed by less than 16°, ranging from 105° to 120°, and remained close to the ideal tetrahedral angle. The coordination number 4 was maintained for both zinc ions in both models.

The two models differ in the protonation state of the inhibitor carboxyl group. The interaction of this residue with Lys161 was investigated. In the crystal structure, the arithmetic mean of the distances between the inhibitor carboxyl oxygens and the Lys161 side chain nitrogen is 3.1 Å, indicating a salt bridge. The distances between the two carboxyl oxygens and the Lys161 nitrogen were monitored over the course of the simulations (Figure 5). At the beginning of both simulations, the arithmetic mean of the distances between either carboxyl oxygen and the Lys161 nitrogen was 3-4 Å. This distance remained stable during the 1.75 ns simulation of the model with protonated inhibitor (Figure 5A), indicating a stable salt

bridge. In the simulation with deprotonated inhibitor, the distance was stable during the first 950 ps, but then it abruptly increased to values of 7-10 Å (Figure 5B), indicating a breakdown of the salt bridge, and the carboxylate then pointed towards Asn167 and the side chain of Trp28.

## Free IMP-1

In a model of the free enzyme using the cationic dummy atom method, a hydroxide was positioned as a bridging ligand between the two zincs. The structure was stable in a MD simulation at 300 K for 1 ns (Figures 6A and B). The Zn1-Zn2 distance fluctuated around 3.65 Å. A tetrahedral coordination of both zincs with the initial amino acid ligands was maintained (zinc-ligand distances: 1.9-2.1 Å, ligand-zinc-ligand angles: 100-115°).

## IMP-1 in complex with substrate

A well converted cephalosporin, cephalothin, was docked into the active site of IMP-1 in an intermediate structure as suggested recently for the *Bacteroides fragilis* metallo-β-lactamase (Wang *et al.*, 1999). Both enzymes have 29% sequence identity, and their active sites are identical. In contrast to the proposed mechanism, we deprotonated the carboxyl group of the substrate resulting from hydrolysis of the amide bond and protonated the carboxyl group on the six-membered ring of cephalothin (Figure 1), because in a simulation where the latter was deprotonated, it replaced zinc ligands, mainly the anionic nitrogen (data not shown). For 1.2 ns of MD simulation, the complex was stable (Figure 6C) and the geometry of the substrate-protein complex was maintained (Figure 7). After 1.4 ns, however, the distance between Lys161 and the carboxyl group at the six-membered ring of cephalothin increased and, accompanied by a flip of the six-membered ring, the dihydro thiazine sulfur atom replaced the

anionic nitrogen, which then lost contact to Zn2. In the still intact average structure over 10 ps after 1.2 ns of simulation (Figure 7), the ligand-zinc distances were between 1.9 and 2.2 Å and the ligand-zinc-ligand angles between 99° and 116°. The initial coordination of both zinc ions was maintained throughout the 1.2 ns. Up to that point, the arithmetic mean of the distances between the two carboxyl group oxygens of the substrate and the Lys161 side chain nitrogen was 3-4 Å, and the Zn1-Zn2 distance increased by about 1 Å to ~4.6 Å (Figure 6D) compared to the crystal structure with inhibitor.

It has been suggested that Asn193 in the *Bacteroides fragilis* metallo-β-lactamase might stabilize the substrate intermediate by interacting with the carboxyl group resulting from the amide bond hydrolysis (Wang *et al.*, 1999). To test this assumption, the distance between the side chain nitrogen of the corresponding Asn167 in IMP-1 to the carboxylate resulting from hydrolysis of the β-lactam was measured during the course of the simulation. During 1.2 ns of simulation, it had steadily increased from 5.3 Å to about 12 Å (Figure 6E).

# Discussion

## Quality of the models for IMP-1 in complex with inhibitor

$Zn^{2+}$ is a transition metal with $d^{10}$ configuration, one empty *s* and three empty *p* orbitals in the outer electron shell. In the presence of four ligands, the formation of four tetrahedrally arranged $sp^3$ hybrid orbitals would be expected, which can accommodate electron density and result in tetrahedral coordination. This geometry is also observed in the protein environment (Concha *et al.*, 2000).

With a purely nonbonded approach, the coordination number increased during the MD simulation and the tetrahedral coordination was not maintained. In such a model, the electrostatic interactions between zinc and its ligands are not directed, and the positively charged zinc ion pulls all potential ligands into its first coordination sphere. This approach would be appropriate to model a system of four ligands. However, in a complex protein environment, numerous amino acids with a negative charge and sufficient flexibility may function as ligands. The entry of additional ligands like glutamic and aspartic acids into the first coordination sphere has been reported using the *AMBER* and the *CHARMM* force field (Hoops *et al.*, 1991; Stote and Karplus, 1995; Pang *et al.*, 2000; Pang, 2001). In the purely nonbonded model investigated here, such a movement has been observed for the second oxygen of Asp81 and the inhibitor carboxylate. Apart from these acidic moieties, Cys158 coordinated not only to Zn2, but also to Zn1 during the simulation, and Ser196 entered into the first coordination sphere of Zn2 (Figure 3). Using the cationic dummy atom approach (Pang *et al.*, 2000), this problem could be circumvented. The tetrahedral coordination of the zinc atoms was kept throughout the MD simulations. Asp81 stayed coordinated to Zn2 with only one oxygen and Cys158 remained coordinated only to Zn2, but not to Zn1 (Figure 4). This is probably due to a more directed electrostatic interaction between ligand and transition

metal atom using this method. There is a minor force pulling other potential ligands close to the zinc atom, because each dummy atom has a partial charge of +0.5 e and is paired to a negatively charged ligand. It should be mentioned that it was necessary to deprotonate the ligands in this model. Simulations with neutral histidines were also performed, but in the course of the simulation they lost contact to the dummy atoms (data not shown).

The purely nonbonded approach models zinc with a charge of +2 e and neutral histidines. This leads to a strong electrostatic repulsion of the two zinc ions and an increase of their distance by 1.1 Å compared to the experimental structure. This effect was also observed for a phosphotriesterase with a binuclear zinc metal center when using a purely nonbonded approach (Pang, 2001). However, in the complex a delocalization of electron density from the ligands into the vacant $4s4p^3$ metal orbitals takes place, therefore reducing the positive charge there. The cationic dummy atom approach mimics this effect to some extent by delocalizing the positive charge from the center of the metal atom towards the four negatively charged ligands by 0.9 Å. Additionally, the negatively charged histidinates shield the positive charge of the zinc ions. The geometry of the modeled structures (Figures 4) still differed slightly from the crystal structure (+0.2 Å for the zinc-zinc distance and –0.2 Å for the ligand-zinc distances in average). However, taking into account the resolution of 2.0 Å of the crystal structure, this model can be considered a good representation of the IMP-1 metallo-β-lactamase.

In the crystal structure (Concha *et al.*, 2000), a tight interaction was observed between the inhibitor carboxyl group and Lys161. One might expect that treating the inhibitor carboxyl group as deprotonated resulted in a better model than treating it as protonated, thus allowing stronger electrostatic interactions between this residue and the positively charged Lys161. In contrast to this expectation, the carboxylate lost contact to Lys161 after 950 ps of simulation and then pointed towards Asn167 and Trp28. Similar as in the purely nonbonded model, where $Zn^{2+}$ attracted further ligands, the high negative charge of the carboxylate oxygens

resulted in electrostatic interactions with more distant residues. However, when the carboxyl group of the inhibitor was protonated, it remained oriented towards Lys161 throughout the simulation. In agreement with the cationic dummy atom approach (Pang *et al.*, 2000), this group can be regarded as a second coordination shell ligand, requiring protonation, and also as an acceptor for the thiol proton of the inhibitor.

By comparison of the average structures resulting from the three models as summarized in Table 1, we conclude that the cationic dummy atom approach with protonated inhibitor gives the best representation of the crystal structure.

## Extension of the cationic dummy atom model to the free enzyme and substrate-bound enzyme

In Table 2, the geometric parameters measured in the modeled structures of the free enzyme and IMP-1 in complex with cephalothin are compared. The very similar structure of the *Bacteroides fragilis* metallo-β-lactamase has been crystallized as a free enzyme (PDB entry 1ZNB, resolution 1.85 Å) (Concha *et al.*, 1996). Here, the zinc-zinc distance was 3.46 Å. Also a crystal structure of IMP-1 as free enzyme is available (PDB entry 1DDK) (Concha *et al.*, 2000) at a resolution of 3.1 Å. In this structure, an acetate is located close to the two zinc ions which have a distance of 3.3 Å. In the modeled structure of IMP-1, this distance was 3.65 Å which is in agreement with the crystal structures. It should be mentioned that in the *B. fragilis* structure Zn2 has a trigonal bipyramidal coordination including a water molecule as additional ligand, whereas in our model it was coordinated tetrahedrally. Interestingly, in the IMP-1 crystal structure with the thiolate as a bridging ligand, the Zn1-Zn2 distance was slightly larger than in the free *B. fragilis* enzyme with hydroxide as bridging ligand (3.6 Å compared to 3.46 Å). In the respective modeled structures of IMP-1, we obtained a corresponding tendency (3.8 Å compared to 3.65 Å). This finding is probably due to the

bigger van der Waals radius (2.0 Å) and the smaller negative partial charge (-0.982 e) of the inhibitor sulfur compared to the hydroxide oxygen (1.77 Å and –1.215 e) used in the simulations.

The protein in complex with cephalothin as an intermediate was modeled without constraints at 300 K for 1.4 ns, but then a conformational change occurred. While in a bonded model this structure might have been stable over a longer period of time, a nonbonded approach is preferable since it has a higher flexibility and thus sensitivity to structural and dynamical effects upon substrate binding. Compared to a purely nonbonded approach the cationic dummy atom approach gives a better representation of the active site. Thus it combines the sensitiveness of the purely nonbonded approach with the correct geometry of the bonded approach at the cost of a reduced long time scale stability of the complex due to electrostatic interactions with more distant atoms. However, the necessary simulation time depends on the equilibration time of the property under investigation (Hansson *et al.*, 2002). In our study the 1.4 ns during which IMP-1 in complex with cephalothin was stable is much longer than the equilibration time in the active site: Zinc-ligand distances, ligand-zinc-ligand angles, and the zinc-zinc distance reached constant values within the first 200 ps (Figure 6D). Mixed bonded and nonbonded models have been used to model the mononuclear *Bacillus cereus* (Díaz *et al.*, 2001) and the binuclear *Bacteroides fragilis* metallo-β-lactamase (Salsbury *et al.*, 2001). However, it is not consistent to treat some ligands as covalently bonded and others as interacting via electrostatic interactions, while all of them are coordinatively bonded to the metal ion. The geometry of the active site of the *Bacteroides fragilis* enzyme in complex with a thiolate inhibitor and as free enzyme was stable (Salsbury *et al.*, 2001). As this protein has 29% sequence identity with IMP-1, the active site is identical and the thiolate inhibitor is very similar to the mercaptocarboxylate inhibitor in structure and binding mode, these simulations can be compared to our simulations. However, they do have a less sensitive active site and the zinc coordination can never change, a property that we are

taking advantage of in determining stability of different enzyme/substrate complexes (Oelschlaeger et al., in preparation). Additionally, it would be difficult to parameterize the active site for an enzyme/substrate complex for a bonded approach, because it undergoes significant changes and the starting structure does not correspond to the structure of the simulated complex.

From the simulations of the free IMP-1 enzyme and the protein in complex with cephalothin, three conclusions can be deduced:

1) The intermediate as proposed by Wang *et al.* (Wang *et al.*, 1999) remained coordinated to both zinc ions during the MD simulation at 300 K over a period of 1.4 ns without any constraints. This finding suggests that this is actually a relevant structure and supports the mechanism of hydrolysis proposed by Wang and coworkers.

2) Our model helps in understanding experimental data obtained with different mutations. Throughout the 1.4 ns of simulation, the substrate carboxyl moiety and Lys161 remained oriented towards each other. Lys161 has been shown to be required for electrostatic interaction with this moiety (Haruta *et al.*, 2001): Mutation of this residue to arginine, alanine or glutamic acid singificantly decreased $k_{cat}/K_M$ values. However, the distance of the Asn167 side chain to the substrate carboxylate resulting from amide bond hydrolysis increased from 5.3 Å to 12 Å during the simulation and suggests that no interaction occurred. While a role of the corresponding residue Asn193 in the *B. fragilis* enzyme in binding of nitrocefin has been proposed (Wang *et al.*, 1999), experimental data by Haruta *et al.* (Haruta *et al.*, 2001) showed that an Asn167Ala mutation had no effect on the hydrolysis of cephalothin. Materon and Palzkill (Materon and Palzkill, 2001) observed that the same mutation showed more efficient hydrolysis of some β-lactam substrates (ampicillin, nitrocefin, cefotaxime, cephaloridine) and concluded that Asn167 is not critical for the binding and turnover of substrates. Our simulation is in agreement with these experimental observations.

3) The increase of the Zn1-Zn2 distance in the substrate complex is very likely due to the absence of a bridging ligand, the hydroxide in the free enzyme or the inhibitor in the IMP-1/inhibitor complex. Quantum-mechanical calculations for *B. fragilis* metallo-β-lactamase (Suarez *et al.*, 2002) indicate that the Zn1-OH-Zn2 bridge broke down and the Zn1-Zn2 distance increased to 4.5-5 Å upon protonation of Asp103, corresponding to Asp81 in IMP-1. This is in agreement with a distance of 4.3–5.2 Å observed in the MD simulation of IMP-1 in complex with cephalothin (Figure 6D). If the bridging ligand is missing, the distance is larger. In contrast, if a bridging ligand is present (free enzyme with hydroxide, enzyme with inhibitor) the Zn1-Zn2 distance is small (3.65 and 3.8 Å, respectively). Consequently, the zinc ions seem to move back and forth by 1 Å during the catalytic cycle. The active site of the binuclear metallo-β-lactamases thus has to be flexible to support this conformational change.

## Conclusions

A model of the IMP-1 enzyme in complex with cephalothin as an intermediate revealed interactions between the protein and the substrate which are in accordance with previous observations obtained in experiments and quantum-mechanical calculations. Therefore, the cationic dummy atom approach, in which the dynamics of the active site is not hindered by covalent bonds and a proper coordination of the zinc ions is maintained, is adequate for MD simulations of this binuclear metallo-β-lactamase.

# Acknowledgement

This work was supported by the German Federal Ministry of Education and Research (project PTJ 31/0312702).

# References

Ambler, R. (1980) *Philos Trans Roy Soc Lond B Biol Sci* **289:** 321-331.

Aqvist, J. and Warshel, A. (1990) *J Am Chem Soc* **112:** 2860-2868.

Berweger, C.D., Thiel, W., and van Gunsteren, W.F. (2000) *Proteins* **41:** 299-315.

Carfi, A., Pares, S., Duee, E., Galleni, M., Duez, C., Frere, J.M., and Dideberg, O. (1995) *Embo J* **14:** 4914-4921.

Case, D.A., Pearlman, D.A., Caldwell, J.W., Cheatham, T.E., III, Ross, W.S., Simmerling, C.L., Darden, T.A., Merz, K.M., Jr., Stanton, R.V., Cheng, A.L., et al. 1999. AMBER Version 6. University of California, San Francisco.

Concha, N.O., Janson, C.A., Rowling, P., Pearson, S., Cheever, C.A., Clarke, B.P., Lewis, C., Galleni, M., Frere, J.M., Payne, D.J., et al. (2000) *Biochemistry* **39:** 4288-4298.

Concha, N.O., Rasmussen, B.A., Bush, K., and Herzberg, O. (1996) *Structure* **4:** 823-836.

Cornell, W.D., Cieplak, P., Bayly, C.I., Gould, I.R., Merz, K.M., Ferguson, D.M., Spellmeyer, D.C., Fox, T., Caldwell, J.W., and Kollman, P.A. (1995) *J Am Chem Soc* **117:** 5179-5197.

Díaz, N., Suárez, D., and Merz, K. (2001) *J Am Chem Soc* **123:** 9867-9879.

Green, D.W. (2002) *Expert Opin Ther Targets* **6:** 1-19.

Hammond, G.G., Huber, J.L., Greenlee, M.L., Laub, J.B., Young, K., Silver, L.L., Balkovec, J.M., Pryor, K.D., Wu, J.K., Leiting, B., et al. (1999) *FEMS Microbiol Lett* **179:** 289-296.

Hansson, T., Oostenbrink, C., and van Gunsteren, W. (2002) *Curr Opin Struct Biol* **12:** 190-196.

Haruta, S., Yamamoto, E.T., Eriguchi, Y., and Sawai, T. (2001) *FEMS Microbiol Lett* **197:** 85-89.

Hawkey, P.M., Xiong, J., Ye, H., Li, H., and M'Zali, F.H. (2001) *FEMS Microbiol Lett* **194:** 53-57.

Heinze-Krauss, I., Angehrn, P., Charnas, R.L., Gubernator, K., Gutknecht, E.M., Hubschwerlen, C., Kania, M., Oefner, C., Page, M.G., Sogabe, S., et al. (1998) *J Med Chem* **41:** 3961-3971.

Hoops, S., Anderson, K., and Merz, K. (1991) *J Am Chem Soc* **113:** 8262-8270.

Huang, C., Lesburg, C.A., Kiefer, L.L., Fierke, C.A., and Christianson, D.W. (1996) *Biochemistry* **35:** 3439-3446.

Hubschwerlen, C., Angehrn, P., Gubernator, K., Page, M.G., and Specklin, J.L. (1998) *J Med Chem* **41:** 3972-3975.

Humphrey, W., Dalke, A., and Schulten, K. (1996) *Journal of Molecular Graphics* **14:** 33-38.

Huntley, J.J., Scrofani, S.D., Osborne, M.J., Wright, P.E., and Dyson, H.J. (2000) *Biochemistry* **39:** 13356-13364.

Kaur, K., Lan, M.J.K., and Pratt, R.F. (2001) *J. Am. Chem. Soc.* **123:** 10436-10443.

Laraki, N., Franceschini, N., Rossolini, G.M., Santucci, P., Meunier, C., de Pauw, E., Amicosante, G., Frere, J.M., and Galleni, M. (1999) *Antimicrob Agents Chemother* **43:** 902-906.

Lee, W., McDonough, M.A., Kotra, L., Li, Z.H., Silvaggi, N.R., Takeda, Y., Kelly, J.A., and Mobashery, S. (2001) *Proc Natl Acad Sci U S A* **98:** 1427-1431.

Liras, P., and Rodriguez-Garcia, A. (2000) *Appl Microbiol Biotechnol* **54:** 467-475.

MacKerell, A.D.J., Bashford, D., Bellott, M., Dunbrack, R.L.J., Evanseck, J.D., Field, M.J., Fischer, S., Guo, J., Ha, S., Joseph-McCarthy, D., et al. (1998) *J Phys Chem B* **102:** 3586-3616.

Matagne, A., Lamotte-Brasseur, J., and Frere, J.M. (1998) *Biochem J* **330:** 581-598.

Materon, I.C., and Palzkill, T. (2001) *Protein Sci* **10:** 2556-2565.

Merz, K.M., Murcko, M.A., and Kollman, P.A. (1991) *J Am Chem Soc* **113:** 4484-4490.

Mollard, C., Moali, C., Papamicael, C., Damblon, C., Vessilier, S., Amicosante, G., Schofield, C.J., Galleni, M., Frere, J.M., and Roberts, G.C. (2001) *J Biol Chem* **276:** 45015-45023.

Ness, S., Martin, R., Kindler, A.M., Paetzel, M., Gold, M., Jensen, S.E., Jones, J.B., and Strynadka, N.C. (2000) *Biochemistry* **39:** 5312-5321.

Pang, Y.P. (1999) *J Mol Model* **5:** 196-202.

Pang, Y.P. (2001) *Proteins* **45:** 183-189.

Pang, Y.P., Xu, K., Yazal, J.E., and Prendergas, F.G. (2000) *Protein Sci* **9:** 1857-1865.

Petrosino, J., Cantu, C., 3rd, and Palzkill, T. (1998) *Trends Microbiol* **6:** 323-327.

Riccio, M.L., Franceschini, N., Boschi, L., Caravelli, B., Cornaglia, G., Fontana, R., Amicosante, G., and Rossolini, G.M. (2000) *Antimicrob Agents Chemother* **44:** 1229-1235.

Roe, R., and Pang, Y. (1999) *J Mol Model* **5:** 134-140.

Ryde, U. (1995) *Proteins* **21:** 40-56.

Salsbury, F.R., Jr., Crowley, M.F., and Brooks, C.L., 3rd. (2001) *Proteins* **44:** 448-459.

Stote, R.H., and Karplus, M. (1995) *Proteins* **23:** 12-31.

Suarez, D., Brothers, E.N., and Merz, K.M., Jr. (2002) *Biochemistry* **41:** 6615-6630.

Suárez, D., and Merz, K. (2001) *J Am Chem Soc* **123:** 3759-3770.

Terp, G.E., Christensen, I.T., and Jorgensen, F.S. (2000) *J Biomol Struct Dyn* **17:** 933-946.

Toba, S., Colombo, G., and Merz, K.M. (1999) *J Am Chem Soc* **121:** 2290-2302.

Toney, J.H., Fitzgerald, P.M., Grover-Sharma, N., Olson, S.H., May, W.J., Sundelof, J.G., Vanderwall, D.E., Cleary, K.A., Grant, S.K., Wu, J.K., et al. (1998) *Chem Biol* **5:** 185-196.

Toney, J.H., Hammond, G.G., Fitzgerald, P.M., Sharma, N., Balkovec, J.M., Rouen, G.P., Olson, S.H., Hammond, M.L., Greenlee, M.L., and Gao, Y.D. (2001) *J Biol Chem* **276:** 31913-31918.

Tainer, J.A., Getzoff, E.D., Beem, K.M., Richardson, J.S., and Richardson, D.C. (1982) *J Mol Biol* **160:** 181-217.

van Gunsteren, W.F., and Berendsen, H.J.C. (1977) *Mol Phys* **34:** 1311-27.

Vedani, A., Dobler, M., and Dunitz, J.D. (1986) *J Comp Chem* **7:** 701-710.

Vedani, A. and Huhta, D.W. (1990) *J Am Chem Soc* **112:** 4759-4767.

Wang, Z., Fast, W., and Benkovic, S.J. (1999) *Biochemistry* **38:** 10013-10023.

Wasserman, Z.R., and Hodge, C.N. (1996) *Proteins* **24:** 227-237.

Yazal, J., and Pang, Y. (1999) *J Phys Chem B* **103:** 8773-8779.

**Table 1.** Geometry of the crystal structure and the modeled structures of IMP-1 in complex with inhibitor. CDDA: cationic dummy atom approach, MCI: mercaptocarboxylate inhibitor. The distance MCI-COO-Lys161-N refers to the arithmetic mean of the distances between the two oxygen atoms of the inhibitor carboxyl group and the side chain nitrogen of Lys161.

| | Structure | | | |
|---|---|---|---|---|
| | Crystal structure | Purely nonbonded model | CDAA, MCI deprotonated | CDAA, MCI protonated |
| Zn1-Zn2 distance [Å] | 3.6 | 4.7 | 3.8 | 3.8 |
| Ligand-zinc distance [Å] | 2.1-2.4 | 2.7-3.0 | 1.9-2.1 | 1.9-2.1 |
| Ligand-zinc-ligand angle | 100-125° | 67-160° | 105-116° | 105-120° |
| Zinc coordination (Zn1/Zn2) | 4/4 | 5/7 | 4/4 | 4/4 |
| MCI-COO-Lys161-N distance [Å] | 3.1 | 3.2 | 9.4 | 3.7 |

**Table 2.** Geometry of the modeled structures of the free enzyme and the enzyme in complex with cephalothin.

| | Structure | |
|---|---|---|
| | Free IMP-1 | IMP-1 in complex with cephalothin |
| Zn1-Zn2 distance [Å] | 3.65 | 4.55 |
| Ligand-zinc distance [Å] | 1.9-2.1 | 1.9-2.2 |
| Ligand-zinc-ligand angle | 100-115° | 99-119° |
| Zinc coordination (Zn1/Zn2) | 4/4 | 4/4 |

# Figure captions

**Figure 1A.** Mercaptocarboxylate inhibitor coordinatively bonded to both zinc ions.

**B.** Hydrolyzed cephalotin coordinated to Zn1 via the carboxylate and to Zn2 via an anionic nitrogen resulting from amide hydrolysis.

**Figure 2.** Simulation of inhibitor complex by three models (**A, B.** purely nonbonded model of IMP-1 with inhibitor, **C, D.** cationic dummy atom model with deprotonated inhibitor, **E, F.** cationic dummy atom model with protonated inhibitor): RMSD (**A, C, E)** and zinc-zinc distances (**B, D, F)** over the course of the simulations.

**Figure 3.** Comparison of the active site in the crystal structure and the inhibitor complex modeled by the purely nonbonded approach. The crystal structure is colored by atom type (light grey: C, red: O, blue: N, yellow: S, dark grey: zinc ions). In the modeled structure amino acids and zinc ions are blue, the inhibitor is red. Amino acids are displayed as sticks and labeled at the Cα atom, the inhibitor as balls and sticks, and zinc ions as CPK model.

**Figure 4.** Comparison of the active site in the crystal structure and the inhibitor complex modeled by the cationic dummy atom approach. **A.** Simulation with deprotonated inhibitor. **B.** Simulation with protonated inhibitor (coloring as in Fig.3) In **A,** the movement of the carboxylate away from Lys161 is indicated by an arrow.

**Figure 5.** Arithmetic mean of the distances between the two oxygens of the inhibitor's carboxyl group and the Lys161 side chain nitrogen in the cationic dummy atom simulations. **A.** with protonated inhibitor, **B.** with deprotonated inhibitor.

**Figure 6.** RMSD (**A, C)** and zinc-zinc distances (**B, D**) over the course of the simulations; **A, B. c**ationic dummy atom model of free IMP-1, **C, D.** cationic dummy atom model of IMP-1 in complex with cephalothin, **E.** distance between the Asn167 side chain nitrogen and the free oxygen of the cephalothin carboxyl group resulting from amide bond hydrolysis over the course of the simulation of the cationic dummy atom model of substrate-bound IMP-1.

**Figure 7.** The active site of substrate-bound IMP-1 modeled with the cationic dummy atom method (coloring as in Fig.3).

**Figure 1:**

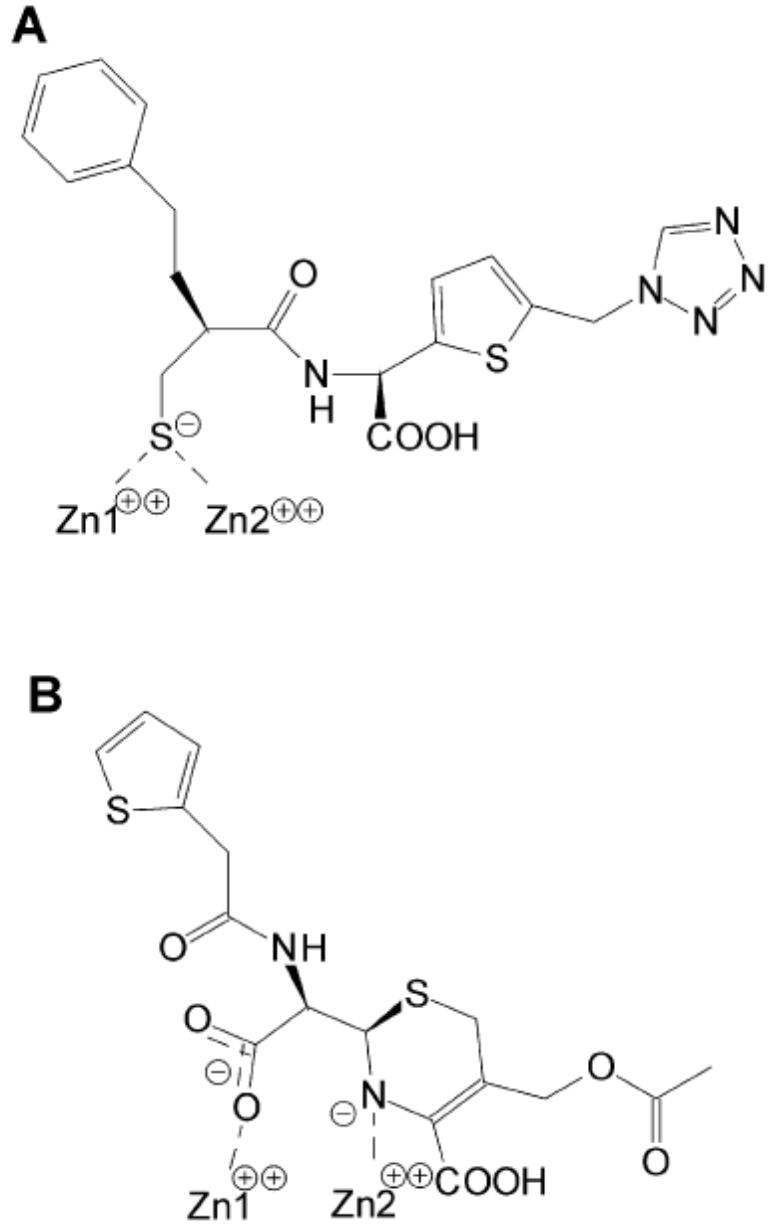

**Figure 2:**

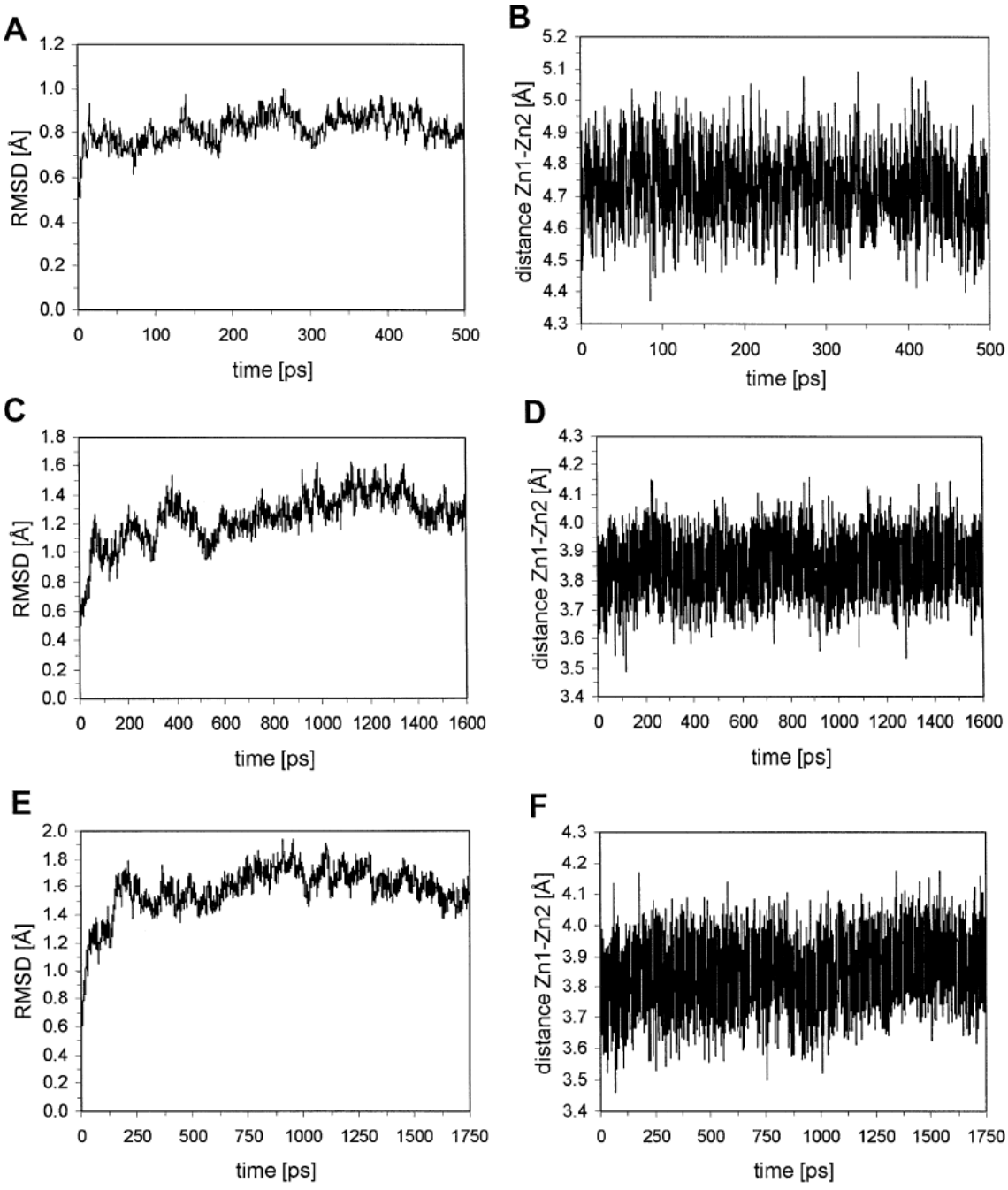
A
RMSD [Å]
time [ps]
B
distance Zn1-Zn2 [Å]
time [ps]
C
RMSD [Å]
time [ps]
D
distance Zn1-Zn2 [Å]
time [ps]
E
RMSD [Å]
time [ps]
F
distance Zn1-Zn2 [Å]
time [ps]

**Figure 3:**

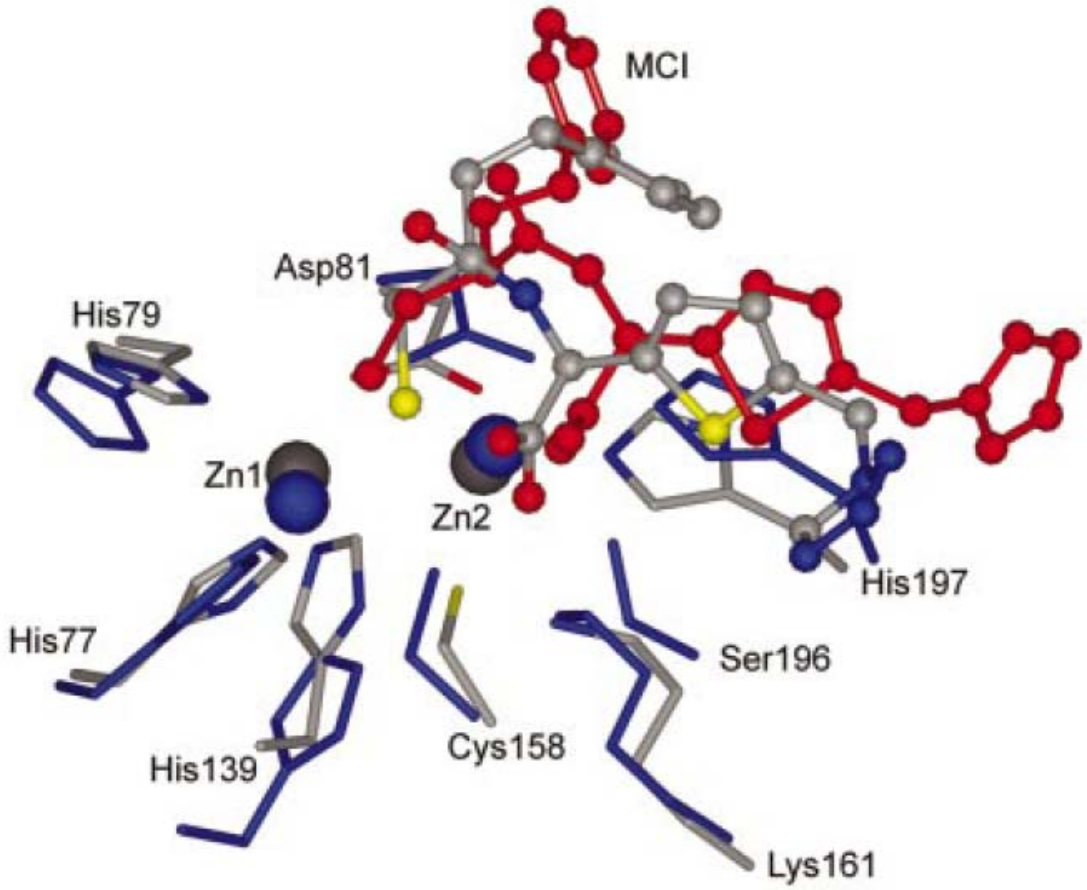


**Figure 4A:**

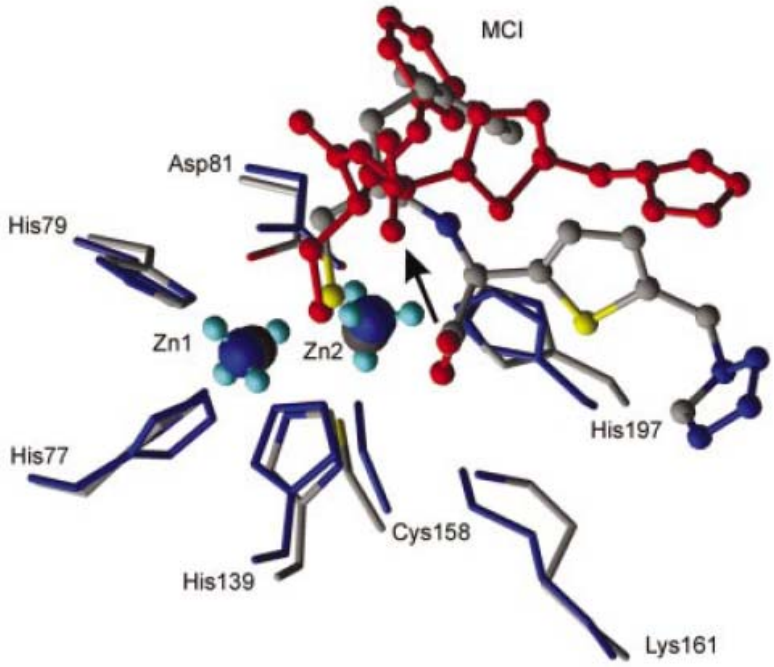

**Figure 4B:**

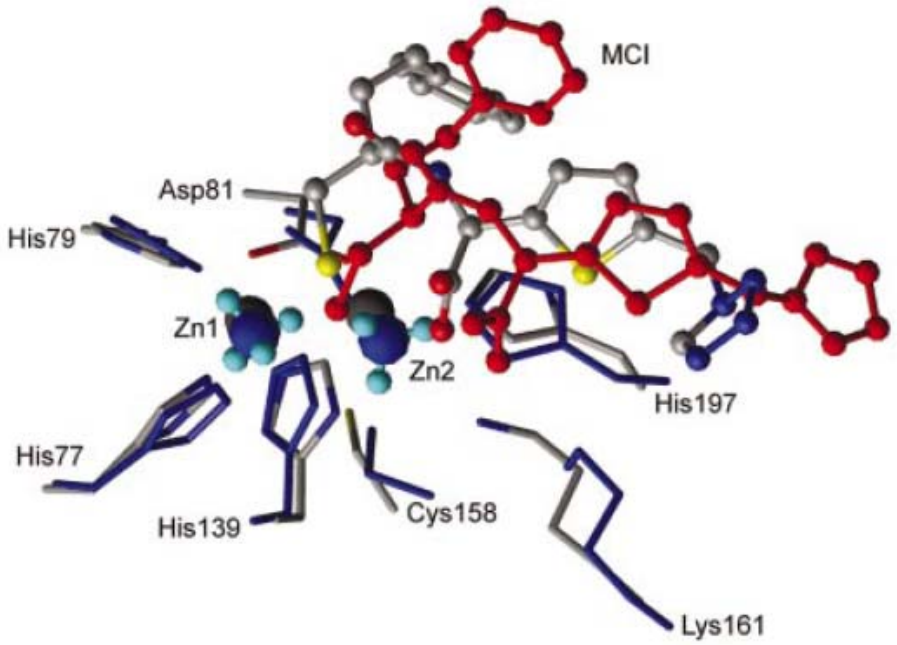


**Figure 5A:**

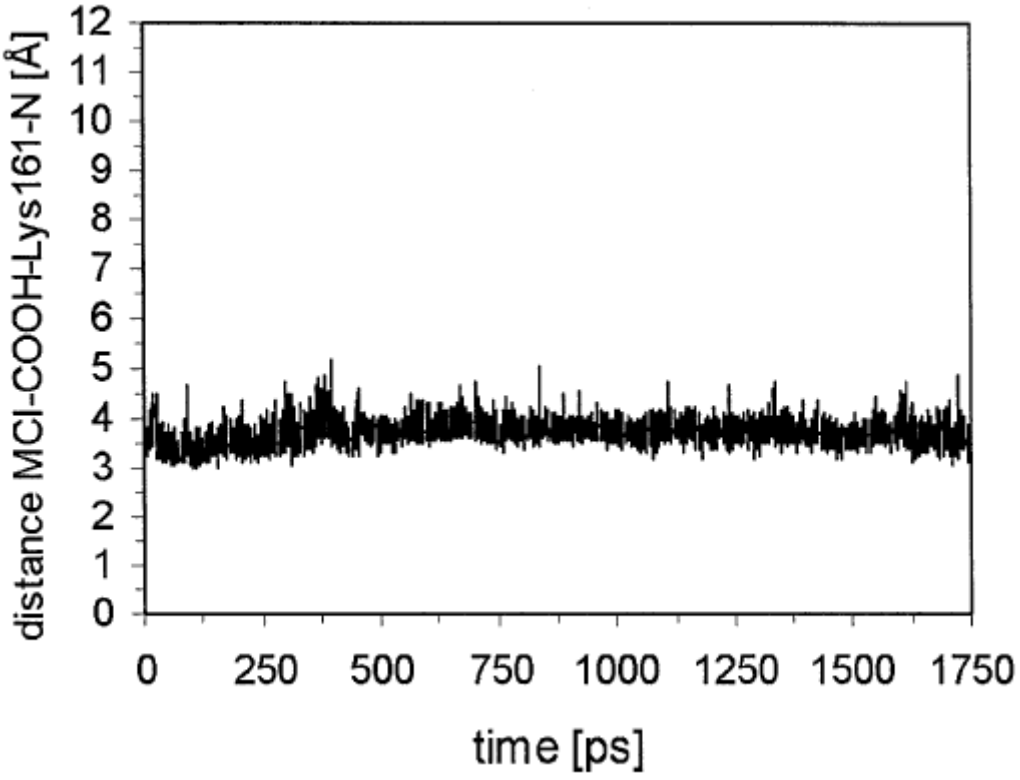

**Figure 5B:**

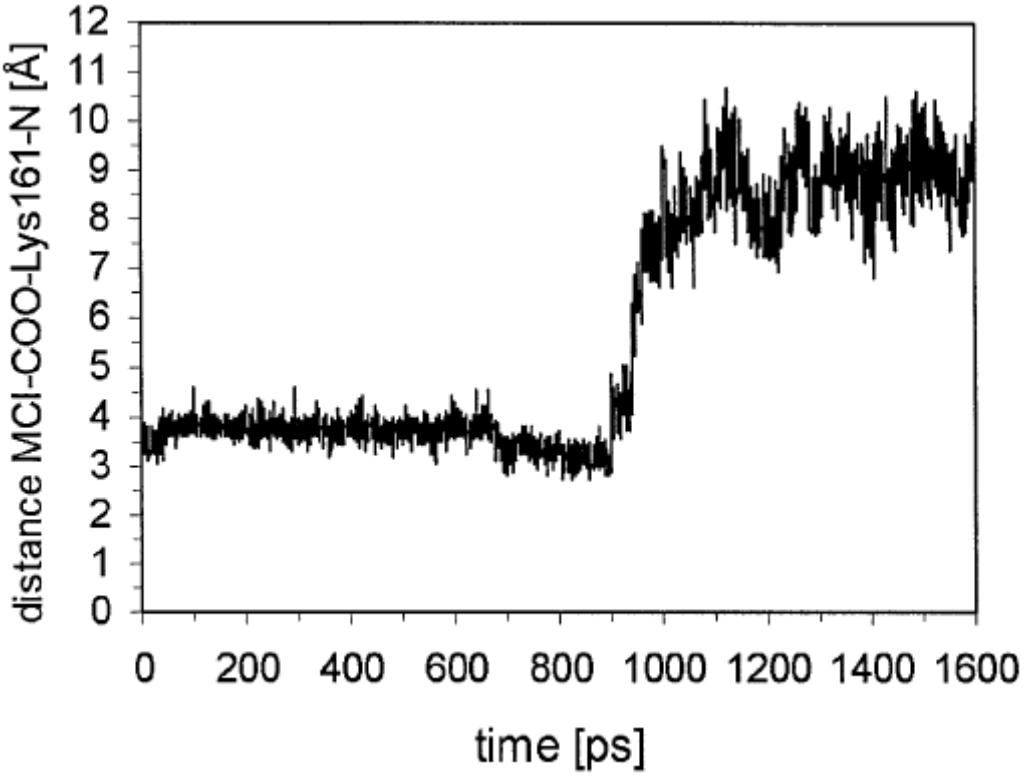
distance MCI-COO-Lys161-N [Å]
0
1
2
3
4
5
6
7
8
9
10
11
12
0
200
400
600
800
1000
1200
1400
1600
time [ps]

**Figure 6:**

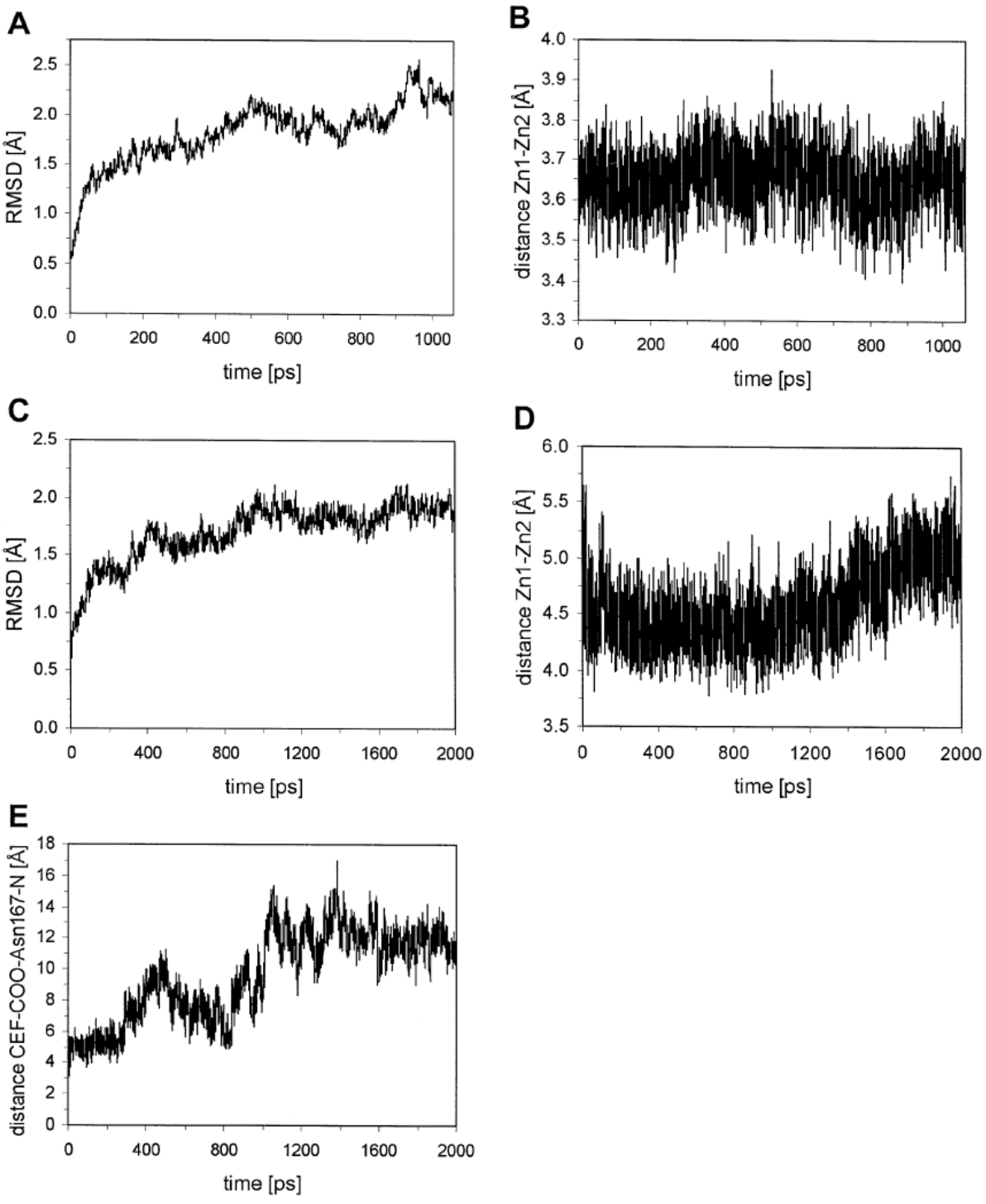
A
RMSD [Å]
time [ps]
B
distance Zn1-Zn2 [Å]
time [ps]
C
RMSD [Å]
time [ps]
D
distance Zn1-Zn2 [Å]
time [ps]
E
distance CEF-COO-Asn167-N [Å]
time [ps]

**Figure 7:**

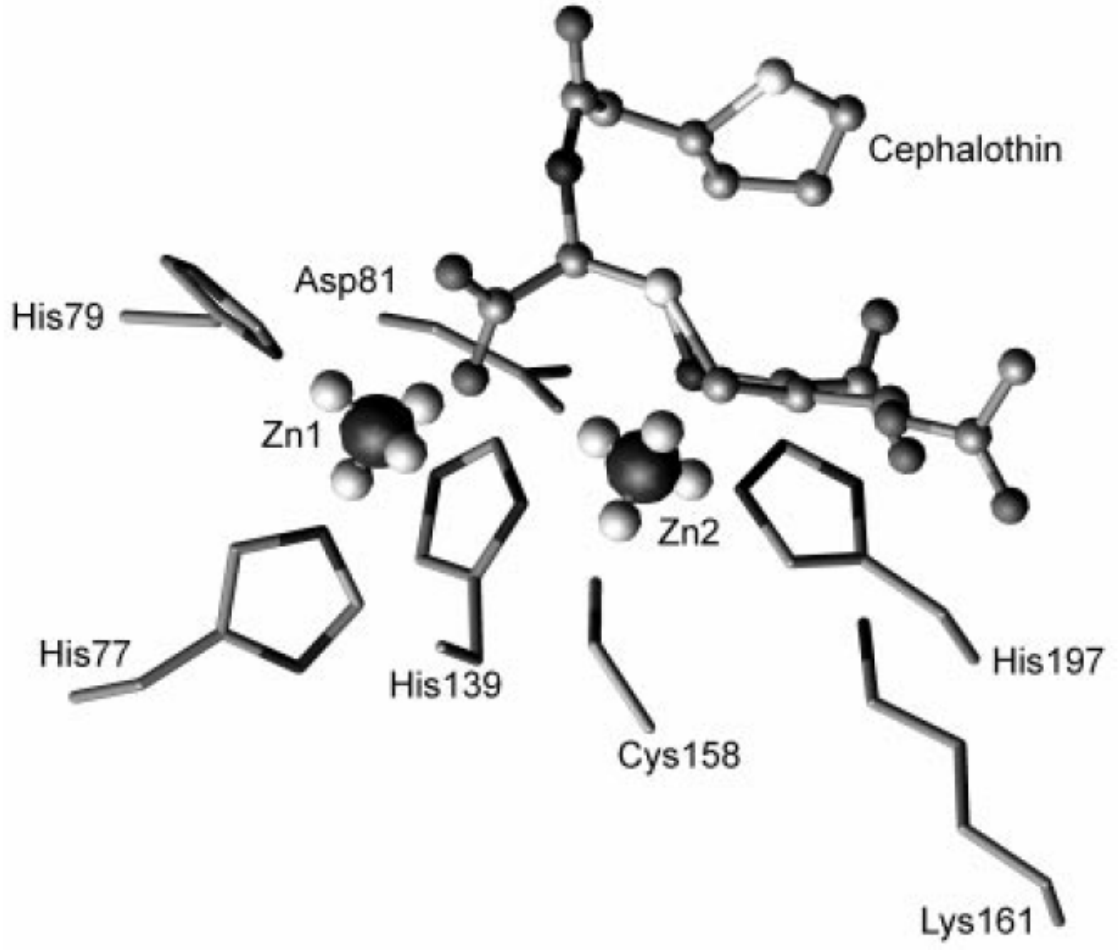
Cephalothin
Asp81
His79
Zn1
Zn2
His77
His139
Cys158
His197
Lys161